

Charge effect in S enhanced CO adsorption: A theoretical study of CO on Au, Ag, Cu, and Pd (111) surfaces coadsorbed with S, O, Cl, and Na

Li-Yong Gan and Yu-Jun Zhao^{a)}

Department of Physics and School of Material Science and Engineering, South China University of Technology, Guangzhou 510640, People's Republic of China

(Received 9 June 2010; accepted 5 August 2010; published online 3 September 2010)

The extraordinary sulfur enhanced CO adsorption on Au surface creates curiosity to many scientists in the field, and is expected to have potential applications in catalyst design. In this work, we have investigated the interactions of the coadsorption of CO and various adatoms X (X=Na, S, O, and Cl) on Au and Pd(111) surfaces and made further comparison with CO adsorption on charged Au and Pd surfaces by a first-principles study. We find out that the enhancement of CO adsorption by S on Au originates from S-induced positive polarization of Au surface. The d band of metal atoms in the positively polarized Au surface shifts up toward the Fermi level (E_F) without remarkable changes of its shape and occupation. In contrast, in the negatively polarized Au(111) surface, achieved by electropositive adatom such as Na adsorption or artificially adding additional electrons to the substrate, d bands shift down relative to E_F , and thus CO adsorption is weakened. Further study of CO coadsorption with X on two other noble metal (Ag and Cu) surfaces manifests that Ag shows the same behavior as Au does, while the situation of Cu is just between that on Au and Pd. It suggests that the extraordinary S-induced enhancement of CO adsorption on Au/Ag, different from other transition metals (TMs), ultimately results from the inertness of d bands buried below E_F . The S-induced charge can introduce a significant d band shift on Au/Ag with respect to E_F due to their narrow density of states at E_F and thus strengthens CO adsorption subsequently. © 2010 American Institute of Physics. [doi:10.1063/1.3483235]

I. INTRODUCTION

The interaction between adsorbates such as atoms, molecules, and ions on metal surfaces is a key to understanding catalyzed reactions on metals. Coadsorbed species on metal surfaces can interact with each other directly due to the overlap of wave functions or through induced dipole-dipole electrostatic interactions or indirectly via the substrate metal d band structure.¹ These interactions between coadsorbates may prefer or exclude a certain reaction pathway or even give rise to a coadsorption complex, enhancing the reactivity and controlling the selectivity as a “promoter”^{2–6} or reducing and even quenching the reaction rate adversely as a “poisoner.”^{7–10}

Gold (Au) has long been considered as being chemically inert.¹¹ In 1987, however, Haruta and co-workers discovered that highly dispersed gold nanoparticles on reducible metal oxide supports catalyzed CO oxidation at a temperature as low as 200 K,¹² leading to a huge number of studies to trace the understanding of the high catalytic performance on gold nanoparticles, particularly the high catalytic selectivity.^{13–16} It is generally agreed that nanoparticles with low-coordinated sites may play a key role in the high catalytic activity of gold-based catalysts.^{17–22} Other factors, such as support interactions^{6,23} and charge transfer,^{24,25} may also be responsible for its high activity. This high catalytic performance has earned Au-based catalysts a reputation of potential green

catalysts,^{26,27} distinguishing them from other traditional transition (TM) catalytic metals, such as Pd and Pt.

On the other hand, the sulfur (S) poisoning effects have been a hot topic in heterogeneous catalysis over several decades^{7,28–33} due to its remarkably negative effects on the reactivity and selectivity of supported metal catalysts.^{29,34,35} In order to understand the S poisoning effects, many experimental and theoretical studies have been carried out^{8,33,36–38} and conclude that S poisoning effect mainly shows a combination of steric (or structural) effects and electronic effects. The former generally describes S blocking contiguous adsorption sites needed by other species, displaying a short-range effect, whereas the latter is associated with charge redistribution or hybridization (i.e., sp or sd), e.g., density of states (DOS) near the Fermi level is substantially reduced by S,^{7,31} showing a long-range influence. The two effects destabilize adsorption of reactants and subsequently hinder the formation of products. However, these destabilization effects, normally found on traditional TM catalysts, “disappear”^{39,40} unexpectedly on the Au(111) surface. Interestingly, the presence of S could also lower the barrier of H₂O dissociation on the Au(111) surface.⁴¹ Through secondary ion mass spectrometry, Mohapatra *et al.*⁴² observed that on Au/TiO₂ catalysts, room-temperature oxidation of CO can be dramatically enhanced by the addition of sulfate ions. These extraordinary novel phenomena once more distinguish Au-based catalysis from other traditional TM catalysts. Besides these, analogous phenomena were observed on the Ag(111) noble metal as well.⁴³ It was found that CO can be

^{a)}Author to whom correspondence should be addressed. Tel.: +86-20-87110426. FAX: +86-20-87112837. Electronic mail: zhaoyj@scut.edu.cn.

stabilized at 90 K on Ag(111) by coadsorbed Cl atoms. Unfortunately, the picture of S promotion effects on Au is still under controversy. Zhang *et al.*³⁹ argued that the enhanced adsorption of CO by these electronegative species may be due to antiparallel molecular dipole interactions, although no large antiparallel dipoles associated with the adatoms were found when CO adsorbs on Au(111) with O, S, or Cl on the fcc hollow sites. On the other hand, Xue *et al.*⁴¹ supposed that the promotion on H₂O dissociation might be ascribed to a strong electron transfer from S to the Au(111) surface.

Obviously, many questions are still open regarding the promotion effect of S; for example, how do S, O, and Cl enhance CO adsorption? Why does the promotion occur on Au and Ag surfaces, but not others? To this end, we perform an extensive density functional theory (DFT) calculations to compare CO adsorption on X (X=Na, S, O, and Cl) preadsorbed Au, Pd, and the other two noble metal surfaces, Ag and Cu(111), aiming to get an insight into the novel phenomenon.

Allowing for the pronounced charge transfer between coadsorbate X and the substrate,^{40,44,45} we have also performed calculations with charged metal substrates. Namely, we add one electron to the surface to make a “negative surface” or remove one or two electrons from the surface to make a “positive surface,” namely, Au^δ and Pd^δ (δ=1−, 1+, and 2+). This is a significant charging ($\sim 10^{-2}$ C/Å²) but is assumed not to affect the most preferred adsorption configurations on each metal surface. As a result, the positively charged Au(111) binds with CO more strongly than neutral Au(111) does, suggesting that the charge transfer between X and Au(111) is responsible for the observed enhancement of CO adsorption on the Au(111) surface.^{39,40} Further investigation indicates that these unique observations on Au and Ag ultimately originate from their deep buried *d* levels and low DOS at *E_F*. The *d* bands remain intact after adsorbing electronegative species, while the preadsorbed X-induced tiny charge transfer can result in a significant shift of Au (Ag) *d* bands with respect to *E_F*, which affects CO adsorption subsequently.

II. CALCULATIONAL DETAILS

This work is conducted by the Vienna *ab initio* simulation package (VASP)^{46–49} with the frozen-core projector-augmented-wave method.^{50,51} The Perdew–Wang (PW91) generalized gradient approximation^{52,53} functional was employed for the exchange–correlation energy. All surfaces are modeled with a five-layer slab with a vacuum thickness of 15 Å. The adsorbed species are placed on one side of the slab. The three uppermost layers are fully relaxed, while the two bottommost layers are fixed at their bulk structure. A cutoff energy of 500 eV is employed in this work. A 3×3 supercell is used to simulate X (X=Na, S, O, and Cl) and CO coadsorption on Au(111) and Pd(111) surfaces (in Fig. 1) and CO adsorption on charged metal surfaces. We employed Monkhorst–Pack k-point grids of 5×5×1 for each 3×3 surface unit cell. The lattice constant of Au bulk was determined to be 4.18 Å, within $\sim 2.5\%$ deviation from the experimental value (4.08 Å), while the lattice constant of Pd

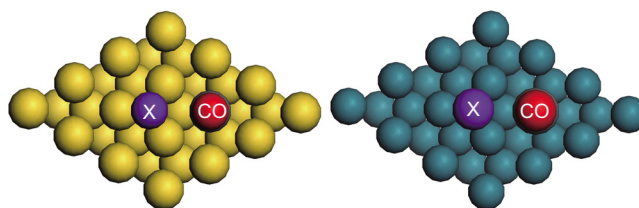


FIG. 1. Coadsorption of CO and X on Au(111) (left) and Pd(111) (right) surfaces, respectively.

bulk was fully optimized to 3.96 Å, within an error of 2% to the experimental value of 3.89 Å.⁵⁴ To imitate CO adsorption on charged Au and Pd surfaces, we add one or remove one or two electrons in the slab, namely, Au^δ and Pd^δ (δ=1−, 1+, and 2+), and the dependence of CO adsorption on the number of substrate layers is strictly tested. For more details, see the Appendix.

The coadsorption energy of CO on X (X=Na, S, O, and Cl) preadsorbed metal surfaces is defined as follows:

$$E_{\text{ad}} = -(E_{\text{CO/X-M}} - E_{\text{X/M}} - E_{\text{CO}}), \quad (1)$$

where $E_{\text{CO/X-M}}$, $E_{\text{X/M}}$, and E_{CO} are the energies of CO and X coadsorbed metal surfaces, X preadsorbed metal surfaces, and CO molecule in the gas phase, respectively. Based on structural results for CO on the two studied surfaces in Ref. 40, the coadsorption is modeled with X preadsorbed at a fcc hollow site on both metal surfaces with CO at the next nearest top site on Au(111) and the nearest fcc site on Pd(111), as shown in Fig. 1.

III. RESULTS AND DISCUSSION

A. CO adsorption on X preadsorbed and charged Au(111) surfaces

Electronegative species enhanced adsorption of CO on the Au surface is a very extraordinary phenomenon different from most TM surfaces. It is argued that NO₂ enhancement may result from the two antiparallel molecular dipole interactions.³⁹ However, single electronegative ions such as sulfur and oxygen also demonstrated enhancement of CO adsorption, although no remarkable antiparallel dipoles associated with the adatoms are expected. Meanwhile, one would wonder what the situation will be if electropositive atoms (such as sodium, Na) are introduced instead of the electronegative adatoms. Will the positive Na be an attractive or repulsive center to the CO adsorption? There were many studies about alkali metal promoted CO adsorption on TM surfaces^{55–59} in literature, and the alkali-enhanced synergic charge transfer on CO adsorption can be described as $d \rightarrow 2\pi^*d$, $5\sigma \rightarrow 5\sigma d$, where $2\pi^*d$ and $5\sigma d$ indicate covalent mixed orbitals formed between metal *d* states and the CO $2\pi^*/5\sigma$ states, respectively.⁵⁸ This strengthens metal–CO bonding and substantially weakens C–O bonds.⁵⁵ However, it is in sharp contrast to gold surfaces. The presence of Na adatom will destabilize CO adsorption obviously at the next nearest top site, while the common poisoners, such as S and Cl, enhance CO adsorption (cf. Table I).

The adsorption energy of CO on Na preadsorbed Au(111) is 0.08 eV versus 0.19 eV on clean Au(111). In

TABLE I. Adsorption energies, E_{ad} (eV), C–O bond length, d_{C-O} (Å), and stretching frequency, f (cm^{-1}), of CO on Au and Pd(111) surfaces before and after X adsorption, with models shown in Fig. 1. The subscript letters “t” and “f” indicate adsorption sites atop (second nearest) and fcc (first nearest), respectively.

System	E_{ad} (eV)	d_{C-O} (Å)	f (cm^{-1})
Au–CO _t	0.19	1.15	2053
Au–S _f +CO _t	0.29	1.15	2088
Au–Cl _f +CO _t	0.30	1.15	2084
Au–O _f +CO _t	0.39	1.15	2077
Au–Na _f +CO _t	0.08	1.16	1969
Pd–CO _f	2.04	1.19	1760
Pd–S _f +CO _f	1.68	1.19	1776
Pd–Cl _f +CO _f	1.81	1.19	1766
Pd–O _f +CO _f	1.79	1.18	1818
Pd–Na _f +CO _f	2.31	1.22	1638

order to explain this unusual phenomenon, first, we treat the coadsorbates as two monopoles. However, Bader’s⁶⁰ charge analysis shows that Na and CO are charged with $+0.992e$ and $-0.094e$ ($+1.766e$ on C and $-1.861e$ on O), respectively. Furthermore, in the structure of Na–CO coadsorption, we find that CO tilted toward Na (C atom is away from Na, while O is close to Na) with an angle of 163.9° , and the O–Na distance is a little shorter than the C–Na distance, 3.53 \AA versus 3.66 \AA . In contrast, electronegative species (such as S) show opposite results, not only for the aspect of monopole interaction between the two adsorbates but also for the tilting direction of CO.⁴⁰ The simple analysis from electrostatic interactions indicates that Na should display an attractive center, while electronegative species (S, Cl, and O) display repulsive effects on CO adsorption. Clearly, it does not agree with the actual results listed in Table I.

From Table I, we note that CO adsorption is most enhanced on oxygen preadsorbed Au surface. To provide insight into the Au–X interaction, we first plot the projected density of states on d orbitals (d -PDOS) of Au atoms (before CO adsorption) in O/Au and Na/Au configurations, as shown

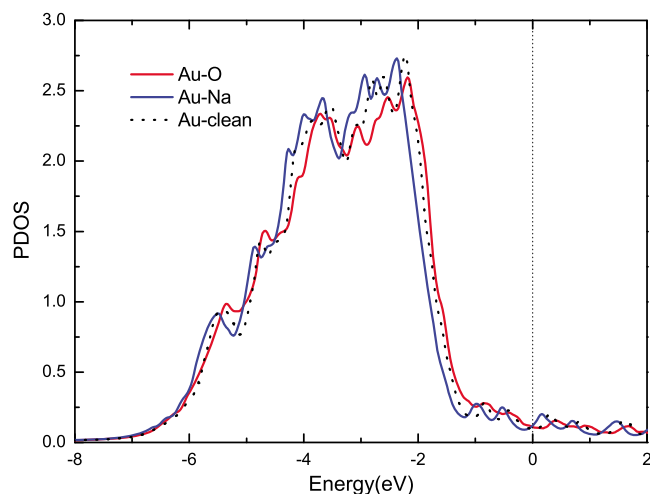


FIG. 2. d -PDOS of the Au atoms in clean Au, O/Au, and Na/Au. The Au atoms employed here are those ready to bond with CO molecule. The Fermi level (E_F) is set to zero.

TABLE II. Adsorption energies, E_{ad} (eV), C–O bond length, d_{C-O} (Å), and stretching frequency, f (cm^{-1}), of CO on the charged Au $^\delta$ and Pd $^\delta$ surfaces ($\delta=2-, 1-, 1+, \text{ and } 2+$). Au 0 and Pd 0 indicate the neutral metal surfaces. The subscript letters “t” and “f” stand for adsorption sites atop and fcc, respectively.

System	E_{ad} (eV)	d_{C-O} (Å)	Charge ^a (e)	f (cm^{-1})
Au 0 –CO _t	0.19	1.15	–0.018	2053
Au $^{1+}$ –CO _t	0.53	1.15	+0.013	2122
Au $^{2+}$ –CO _t	0.87	1.15	+0.038	2143
Au $^{1-}$ –CO _t	0.04	1.15	–0.055	2018
Pd 0 –CO _f	2.04	1.19	–0.029	1760
Pd $^{1+}$ –CO _f	2.06	1.18	+0.009	1818
Pd $^{2+}$ –CO _f	2.12	1.18	+0.052	1861
Pd $^{1-}$ –CO _f	2.06	1.20	–0.067	1724
Pd $^{2-}$ –CO _f	2.10	1.21	–0.104	1670

^aBader charge analysis on clean Au and Pd surfaces.

in Fig. 2. It is clear that the d band of Au surface atom in O/Au shifts up toward the Fermi level, while the d band of Au in Na/Au shifts downward, with respect to that of clean surface. The d band center has been widely regarded as an activity measurement for metals in surface science and catalysis.^{1,61} The closer the d band center (ϵ_d) is to the Fermi level, the easier the charge transfer between the metal surface and the adsorbates, and the higher the activity is. Fortunately, this model can well explain our results—as the d band center shifts up, the adsorption energy of CO increases. Namely, the Au d band shifts upward (downward) to the Fermi level induced by the electronegative (electropositive) atoms, and it subsequently enhances (weakens) the CO adsorption on Au(111).

The Bader analysis indicates that the charges of the Au atoms at the CO adsorption site (before CO adsorption) are $+0.007e$ and $-0.093e$ on O/Au and Na/Au surfaces, respectively, with remarkable changes to that on clean surface ($-0.018e$). Meanwhile, we note that Au atom would become more positively charged as it becomes less coordinated from

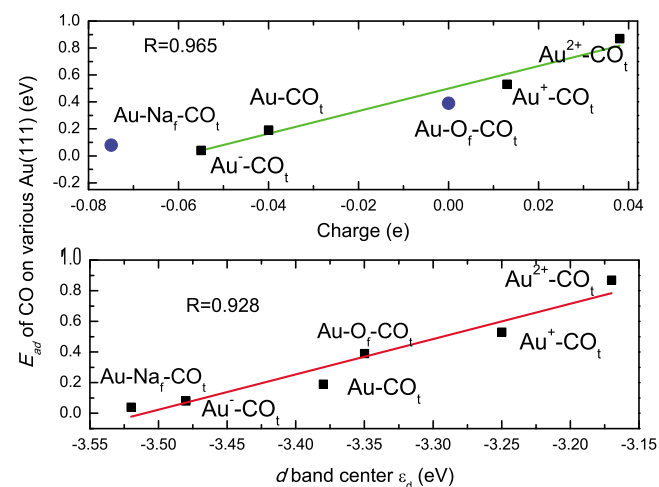


FIG. 3. CO adsorption energies, E_{ad} (eV), vs net charge (upper panel) and d band center (lower panel) of Au atoms ready to bond with CO. Since the effects of O and Na on CO adsorption are the most remarkable, as seen in Table I, only O and Na preadsorbed Au are depicted in the upper panel and emphasized through blue solid circles.

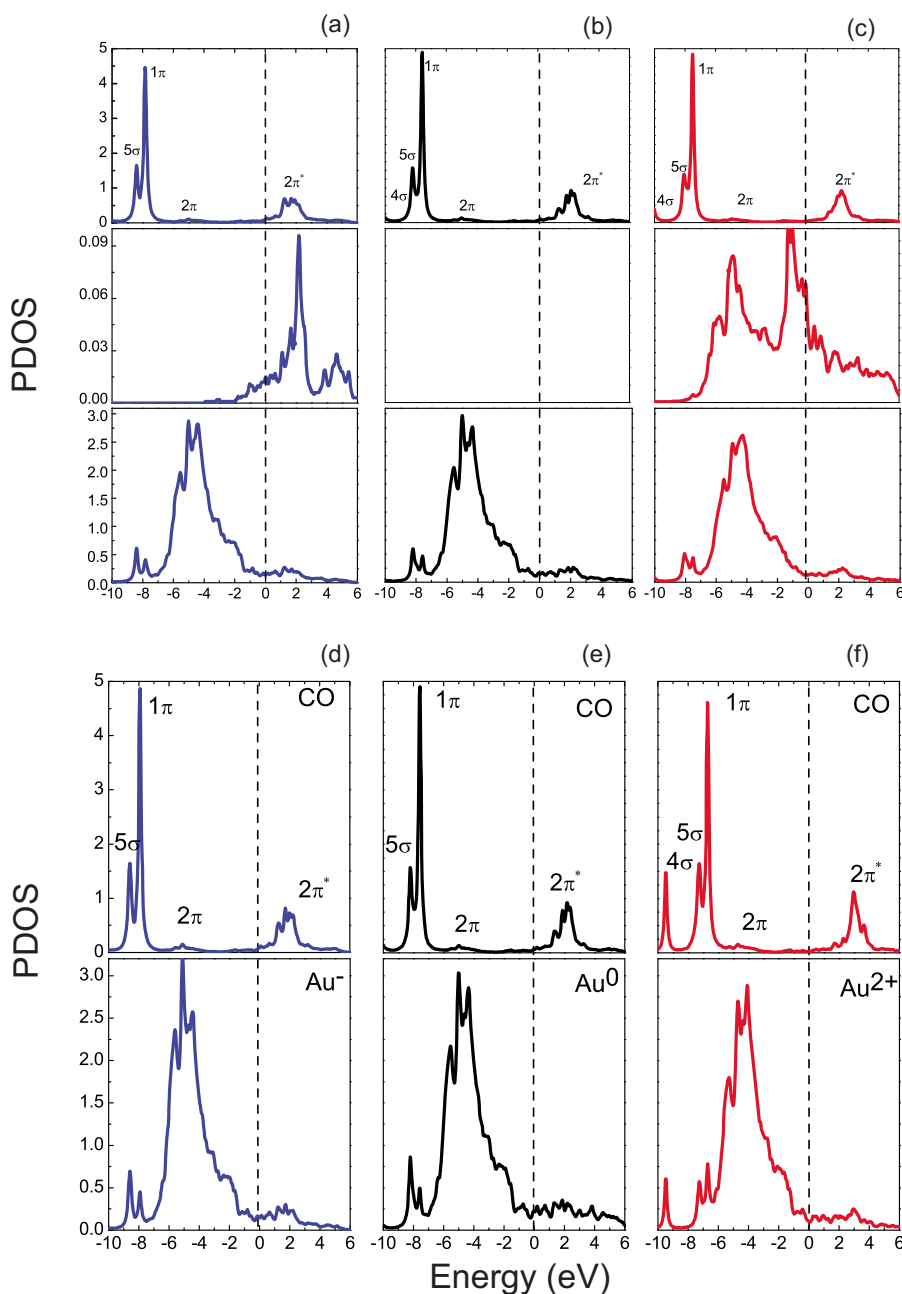


FIG. 4. PDOS of CO adsorbed on Na/Au (a), clean Au (b), S/Au (c), and Au^δ surfaces ($\delta=1-, 1+, \text{ and } 2+$) [(d) and (e)]. The Au atoms employed here are those that bond to CO. The Fermi level (E_F) is set to zero.

Au(111) to Au kinks, with its electron depletion from the s/p levels mainly.¹⁹ That is, its d band filling is kept constant with a corresponding shift of its d band center when the environment of Au atom changes. This provides us a hint that the effects of X (X=O, S, Cl, and Na) on CO adsorption may be dominated by the charge transfer between pre-adsorbed atoms and nearby Au atoms, which introduces a shift of Au d band upward or downward relative to the Fermi level, respectively. To verify it, we performed a systematic calculation of CO adsorption on charged $\text{Au}^\delta(111)$ surface, in which δ equals $1-, 1+, \text{ and } 2+$, meaning to add one to or remove one or two electrons from the neutral clean Au(111) surface per supercell, respectively. The results are listed in Table II. In literature, similar net charge approach by adding electrons to flat surfaces has been used to study the charge

effects of oxygen adsorption on Au(111) surface.⁶² Here, the convergence of net charge approach on CO adsorption on Au(111) surface is carefully tested and further details could be found in the Appendix.

It is obvious that CO adsorption on Au^{1+} and Au^{2+} (111) is much stronger than that on Au^{1-} and Au neutral surfaces. The more positive the polarization of the surface is, the higher adsorption energy of CO will be. Here, one may ascribe that to the interactions between CO dipole and charged surface dipole. However, the dipole interaction is actually repulsive, noting that C atom accumulates positive charge and O accumulates negative charge in CO dipole, and that CO is upright and coordinated via C atom rather than O atom to the substrates. To get an insight into the net charge effect, CO adsorption energies versus net charge and d band center

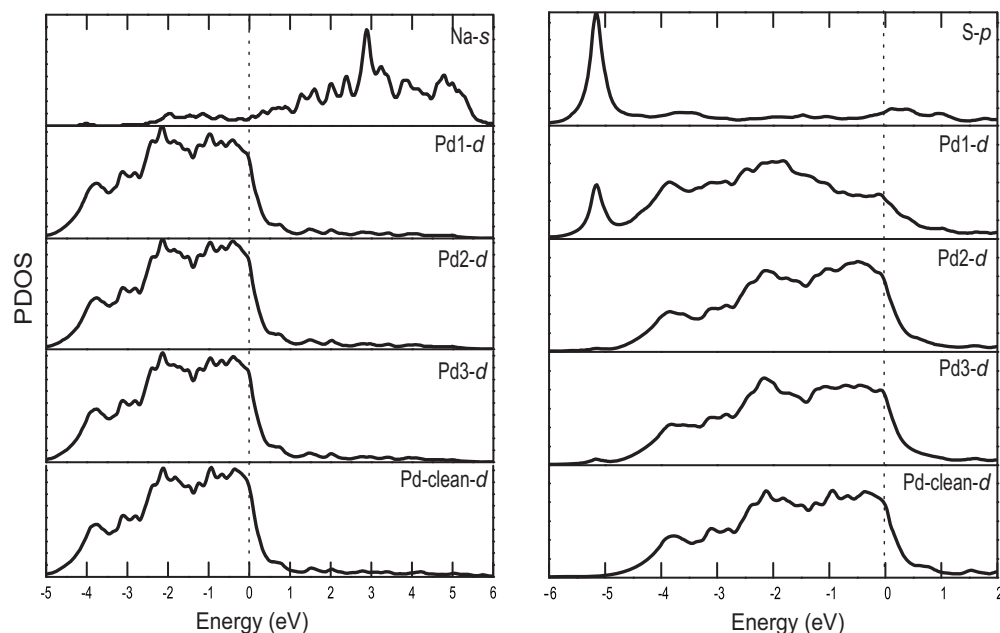


FIG. 5. d -PDOS of the Pd atoms in clean Pd: Na/Pd (a) and S/Pd (b) before CO adsorption. The numbers “1,” “2,” and “3” with “Pd” stand for the first, second, and third nearest neighbor relative to the adatoms (S and Na), respectively. The Fermi level (E_F) is set to zero.

of Au atoms are depicted in Fig. 3. As expected, it illustrates that the d bands of Au shift up toward the Fermi level as the positive charge increases. This can well reproduce the results of CO adsorption on Au–X surfaces. As for CO on Na preadsorbed Au(111) case, the great electrostatic attraction between polarized Na and O stabilizes CO adsorption. Therefore, one can conclude that the extraordinary stabilization by electronegative species and destabilization by electropositive species on CO adsorption on Au(111) mainly result from the Au surface charge effects, namely, negative charge weakens CO adsorption, while positive charge strengthens CO adsorption, as seen in Table II and Fig. 3.

Figure 4 depicts PDOS of CO on S and Na preadsorbed, charged (both positively and negatively), and neutral Au surfaces to further investigate the effects of X and charge on CO adsorption on Au(111) surface. It can be seen that in the upper panels [(a)–(c)], the shape of Au–CO overlap peaks remains almost the same, while the position of these peaks shifts toward or away from E_F slightly due to the presence of Na and S. Na donates its s electron to Au substrate and shifts Au d and CO molecular levels down, leading to a greater occupation in CO antibonding states $2\pi^*$ and subsequently weakens C–O bond with respect to that on clean Au. The C–O bond length and frequency changes accordingly, from 1.16 Å and 1969 cm^{-1} to 1.15 Å and 2053 cm^{-1} . Sulfur, though, shifting these levels up with respect to E_F , results in lower electron occupation in Co $2\pi^*$ and thus strengthens C–O bond, 2088 cm^{-1} (cf. Table I). Effects of S on CO adsorption on Au(111) can be enlarged on positively charged Au(111) surfaces, shown in the lower panels [(d)–(f)] in Fig. 4. It is obvious that all the CO levels move upward further with respect to E_F on positively charged Au(111) surfaces, thus CO $2\pi^*$ are further emptied and the stretching frequencies of C–O on the two positively charged Au surfaces show further blueshifts, 2122 and 2143 cm^{-1} , respectively. From

Fig. 4, it can also be concluded that stabilizing CO on Au with electronegative species results from a higher d band with respect to the Fermi level induced by the charge transfer from Au substrate to the electronegative species.

B. CO adsorption on X preadsorbed and charged Pd(111) surfaces

For a comparison, analogous calculations on Pd(111) surface are conducted. As expected, the presence of Na, like K and Cs on other TM surfaces,^{55–57,59} does stabilize CO adsorption, while the electronegative species weakens CO adsorption on the Pd surface. The calculated results are listed in Table I.

The promotional effect of Na on CO adsorption is evident. The C–O bond length is elongated and the vibration analysis exhibits a redshift on Na preadsorbed Pd surface with respect to that on the clean Pd surface. On electronegative atom preadsorbed Pd surface, however, it is shown that the poisoning effects are not only to weaken CO adsorption but also to strength C–O bond, which will be against the CO-related reactions. Figure 5 shows the difference between the Pd surface preadsorbed with Na and S. It can be seen that the adsorbed Na on Pd will donate its s electron to Pd substrate, but does not influence Pd d band much, as shown in Fig. 5(a). This can no longer be understood through the d band model. We note that once CO adsorbed on Na preadsorbed Pd surface, Na atom will further be ionized, therefore inducing more charge transfer from Na through Pd substrate to the CO lowest unoccupied molecular orbital (LUMO) $2\pi^*$ orbital (not shown in Fig. 5). Upon CO adsorption, Na will be lifted by 0.13 Å, and the distance between Na and O turns out to be only 2.49 Å, while the net charges of Na and O are +0.996 e and –2.005 e , respectively. Besides, the presence of Na shifts the CO levels downward relative to E_F , leading to a further occupation of CO $2\pi^*$. These effects are respon-

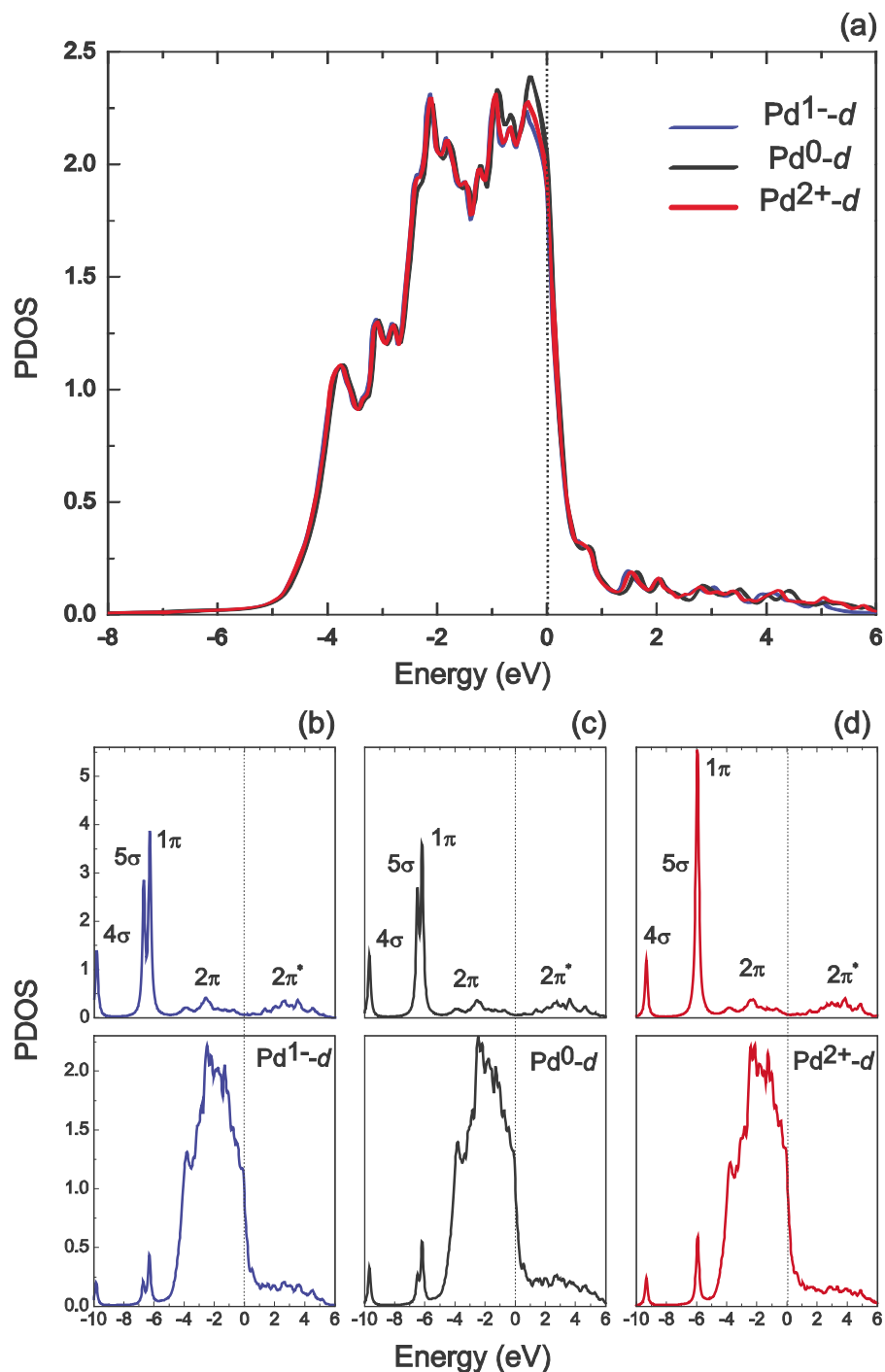


FIG. 6. (a) *d*-PDOS of the Pd atoms in charged and neutral Pd surfaces (Pd¹⁻, Pd⁰, and Pd²⁺) before CO adsorption. [(b)–(d)] PDOS of CO adsorption on Pd surfaces. The Pd atoms employed in the lower panels are those that bond to the CO molecule. The Fermi level (E_F) is set to zero.

sible for the weakening of C–O bond and strengthening of CO–Pd bond.^{58,63} In contrast, in Fig. 5(b), a distinct overlapping between S *p* and Pd *d* could be found -5.2 eV below E_F , suggesting a strong covalent bond between S and Pd substrates. This can substantially increase the *d* band width, lower Pd *d* band center, and reduce DOS near the Fermi level. Different from the Na effects, the S effects on Pd can be extended to the third nearest Pd atoms.⁴⁰

CO adsorption at the adjacent fcc site of Na atom on the preadsorbed Au(111) surface is also studied to compare with that on Pd surface. It is found that CO adsorption is slightly

enhanced by the preadsorbed Na with respect to that on the clean Au(111), 0.22 eV versus 0.15 eV, in line with that of the Na case on Pd(111). Additionally, upon CO adsorption, Na will be lifted by ~ 0.10 Å, and the distance between Na and O is shorter than that of Na and C by 0.37 Å, suggesting that the great electrostatic attraction prevails the negative polarization effect on the Na preadsorbed Au surface. Of note, at the same fcc site on the negatively charged Au¹⁻ surface, E_{ad} of CO is found to be smaller than that on Au neutral surface, 0.10 eV versus 0.15 eV. It indicates that the conclusion drawn in Sec. III A is still valid. On the Na preadsorbed

Pd(111), however, CO adsorption on the top of the second neighbor Pd atom is slightly decreased, 1.40 eV versus 1.43 eV on clean Pd(111). Given the attraction between Na and O, this is similar to that on Na preadsorbed Au surface. Moreover, on both metal surfaces, a similar short-range interaction between Na and CO is observed, in agreement with the recent experimental study.⁶⁴

CO adsorption on charged Pd δ (111) surfaces, with δ of 2-, 1-, 1+, and 2+, is calculated, and the results are listed in Table II. However, unlike that on Au(111) surface, both negative and positive charging hardly affect the CO adsorption energy (within 0.1 eV) on the Pd(111) surface. Negative charging can further weaken C–O, while positive charging strengthens the molecular bond. Consequently, negatively polarized Pd surface may reduce the barrier of CO dissociation, showing higher reactivity with respect to the neutral Pd(111) surface. To understand charging effects on Pd surface atoms and CO adsorption, the *d*-PDOS of Pd atoms in neutral and charged surfaces are plotted in Fig. 6. However, *d* band of Pd surface atoms are hardly influenced by the net charge. The weakened and strengthened C–O bond may be attributed to the dramatic increase (decrease) of occupation in its $2\pi^*$ caused by the negative (positive) charges. All these results are in good agreement with those shown in alkali preadsorbed surfaces,⁶⁵ suggesting that alkali-induced enhancement of CO dissociation may lie in surface negative polarization. Thus, we suggest that some other potential methods can be adopted to negatively polarize Pd surface, as alkali metal does, to enhance its reactivity toward CO and additionally avoid CO blocking effect⁶⁶ and the formation of carbonates⁵⁹ during the process of CO oxidation on alkali metal atom preadsorbed Pd surface.

In fact, charge effects on CO adsorption on Pd are mainly reflected by the shift of CO levels, shown in Figs. 6(b)–6(d). The negative charge shifts these levels downward, while the positive charge raises them toward the Fermi level, especially for the CO bonding state 5σ . It is clear that 5σ and 1π levels can be distinguished easily from each other on the negatively charged Pd(111) surface, while on Pd $^{2+}$ surface, the 5σ state of CO shifts up and almost overlaps with the 1π state. Since the 5σ state is the HOMO of CO, it will be the first to be affected by the positive polarization of Pd surface and thus displays the most remarkable shift. It can be expected that the 5σ level of CO may be further raised toward E_F if Pd surface is further positively polarized.

C. CO adsorption on X preadsorbed Ag and Cu(111) surfaces

Intuitively, analogous studies have been carried out on the other two noble metal (Ag and Cu) surfaces in order to get a deeper understanding of the extraordinary phenomenon on Au surface. We note that it has already been reported that Cl can enhance CO adsorption on Ag(111) surface⁴³ and S introduces a long-range modification to the local density of states (LDOS) of Cu.³³ In the S/Cu case, C–Cu bond is affected by the S-induced LDOS minimum at the second nearest neighbor (NN) adsorption sites and LDOS maximum at the third NN sites. Therefore, CO adsorption at the second

TABLE III. Adsorption energies of CO, E_{ad} (eV), on Ag and Cu(111) surface before and after X adsorption. The subscript letter “t” and “f” indicate adsorption sites, atop and fcc, and “1” and “2” stand for the second and third nearest metal atoms with respect to X, respectively.

System	E_{ad} (eV)
Ag–CO _t	0.11
Ag–S _f –CO _{t1}	0.25
Ag–S _f –CO _{t2}	0.20
Ag–Cl _f –CO _{t1}	0.22
Ag–Cl _f –CO _{t2}	0.2
Ag–O _f –CO _{t1}	0.29
Ag–O _f –CO _{t2}	0.22
Ag–Na _f –CO _{t1}	0.05
Ag–Na _f –CO _{t2}	0.05
Cu–CO _t	0.69
Cu–S _f –CO _{t1}	0.66
Cu–S _f –CO _{t2}	0.71
Cu–Cl _f –CO _{t1}	0.69
Cu–Cl _f –CO _{t2}	0.74
Cu–O _f –CO _{t1}	0.75
Cu–O _f –CO _{t2}	0.73
Cu–Na _f –CO _{t1}	0.62
Cu–Na _f –CO _{t2}	0.62

and third NN atop sites relative to preadsorbed X is considered, and the results are listed in Table III. It indicates that the electronegative species (S, Cl, and O) can stabilize CO adsorption on Ag(111) surface, as observed on Au(111). Furthermore, on both Au and Ag(111) surfaces, the most obvious stabilization occurs on O preadsorbed surfaces. However, the situation on Cu(111) surface is between those on Au and Pd surfaces. CO adsorption is stabilized on O preadsorbed Cu(111) surface, while it is weakened/enhanced at the second/third nearest atop sites on S preadsorbed surface.

D. Further discussion

We have learned that the coadsorption effect on CO adsorption is comparable with that on Au and Ag surfaces, while it is in sharp contrast to that on Pd surface. In the case of Cu surface, the effects are just between those on Au and Pd. This can be understood through the *d* band features of each metal, as illustrated in Fig. 7. The *d* bands of both Au and Ag are buried deep below E_F , and DOS at E_F is extremely narrow, while the *d* bands of traditional TM (such as Pd and Pt) surfaces related to their high activity are often extended to the Fermi level, which pushes up the DOS at E_F . Due to the high DOS at E_F , a tiny charge introduced by the preadsorbed atoms can hardly shift their *d* band centers, exemplified by the case of Na adsorption on Pd(111) surface [cf. Fig. 5(a)] and those of charged Pd surfaces [cf. Fig. 6(a)]. When adsorbing electronegative species, such as S and O, these metals form very strong covalent bonds with adsorbates through their *d* bands. Then the *d* band center shifts down evidently, its width increase accordingly, and meanwhile, the DOS at the Fermi level decreases. That is the negative or poisoning effect^{29,34,35} on TM surfaces, as seen in Fig. 7(a). The negative effects dominate and therefore weaken subsequent CO adsorption.

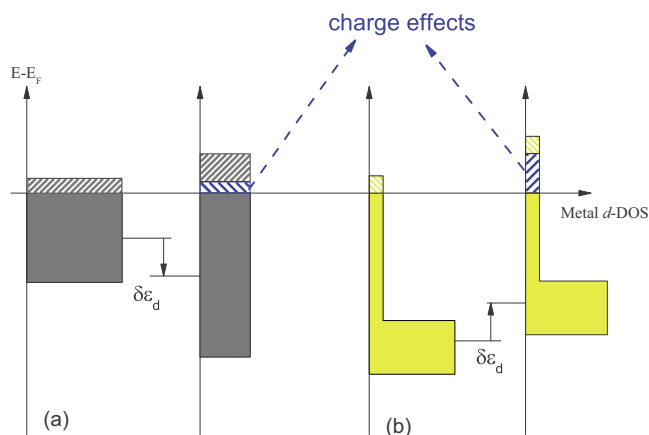


FIG. 7. Sketch of metal d band changes after S, Cl, and O adsorption on TM (a) and on Au or Ag (b). In Au and Ag, the center of d band is shifted up since the charge effects dominate over the poisoning effects, while the poisoning effects prevail on TM. The blue areas indicate the induced charge effects.

On the other hand, noble metals (e.g., Au and Ag) have a narrow DOS at E_F generally due to their d bands buried below E_F . Thus, a tiny charge introduced by the preadsorbed atoms could result in a remarkable shift of the d band relative to E_F and influence the subsequent CO adsorption significantly. Meanwhile, when electronegative species adsorbed on Au or Ag, their impacts on the appearance of metal d bands are not remarkable, while charge effects induced by them, instead, turn to be significant since DOS at E_F is very narrow [cf. Fig. 7(b)]. In other words, on Au or Ag surfaces, electronegative species induced charge effects surpass the negative effects commonly observed on TM surfaces, and thus CO adsorption is enhanced subsequently.

Finally, it should be noted that all shifts of d band mentioned in this article are relative to the Fermi level. They are not the real shifts of d level, but are more likely the shifts of the Fermi level induced by X or charging effects, and result in relative upward and downward movements of metal d bands. Here, we use the shifts of metal d bands directly just for convenience.

IV. CONCLUSION

Extensive DFT calculations of CO adsorption on X (X = O, S, Cl, and Na) preadsorbed and charged Au and Pd surfaces have been carried out and further calculations about CO and X coadsorption on the other two noble metal surfaces are also presented in order to understand the extraordinary enhancement of CO adsorption by electronegative species on Au. We conclude the following.

- (i) Adsorbed electronegative adatoms or positive charging effects shift Au d band up, while adsorbed Na and negative charging effects shift Au d band down, and subsequently affects CO adsorption. The more positive the Au atom is, the higher its d band is relative to the Fermi level, and the stronger CO adsorption will be, in good agreement with those of CO adsorption on X preadsorbed Au(111) surfaces. However, the nega-

tive or positive charging effects on Pd surface have little influence on the d bands of its surface atoms and the CO adsorption.

- (ii) The d bands of Au/Ag are very deep, and thus they will almost remain intact after X adsorption. The narrow DOS at E_F remarkably enhances the X-induced charge effects on the position of d bands. In Au/Ag, electronegative species induced charge effects dominate over the negative effects commonly observed on TM surfaces, and therefore enhance CO adsorption accordingly.

ACKNOWLEDGMENTS

This work was supported by the New Century Excellent Talents Program (Grant No. NCET-08-0202) and the Fundamental Research Funds for the Central Universities, SCUT, under Project No. 2009ZZ0068 and completed with the cooperation of HPC Laboratory, Shenzhen Institute of Advanced Technology, CAS, China.

APPENDIX: CONVERGE TEST FOR CO ADSORPTION ON CHARGED AU SURFACES

Convergence tests have been carried out for CO adsorption on charged Au surfaces with regard to the layers in the slab used in the calculations, given the electrostatic effects on metals. The (1×1) supercell, namely, with CO coverage of 1 ML and an $11 \times 11 \times 1$ k-point mesh, is used in the test.

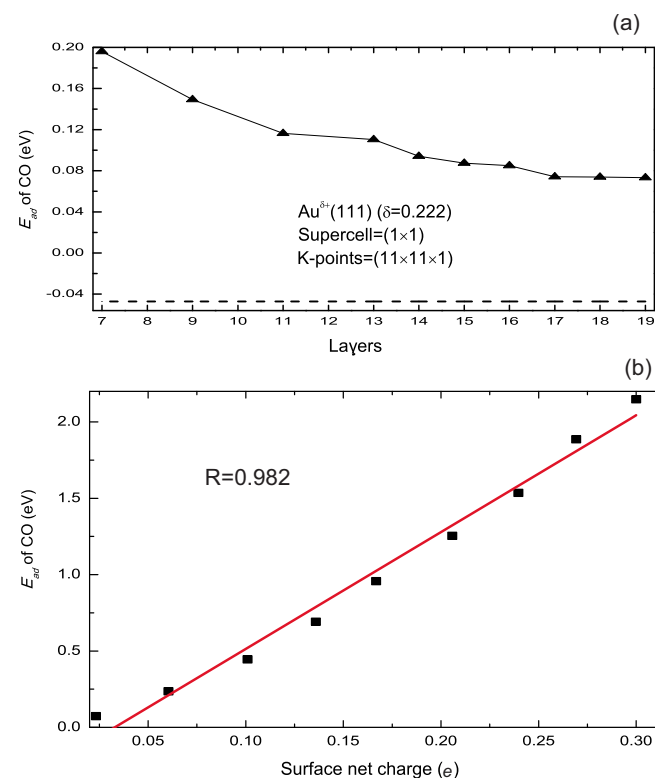


FIG. 8. (a) Convergence test of CO adsorption on the Au surface with a charge of $+0.222e$, with respect to the number of layers in the substrate; with dashed line showing the adsorption energy of CO on neutral Au(111) with the same coverage. (b) CO adsorption energy as a function of the surface net charge with a 17-layer slab model.

In order to decouple the consecutive slabs, a vacuum space with 20 Å is used. Slabs are modeled with symmetric slab geometry structures, and CO molecules are placed on both sides of the slabs. These slabs with different layers are all polarized by $+0.222e$. The dependence of CO adsorption on charged Au surface on layers is presented in Fig. 8(a). It can be seen that the adsorption energy of CO on the charged Au surfaces converges completely at the substrate of 17 layers, and the adsorption is obviously stronger than that on neutral Au surface.

We also calculated CO adsorption energy as a function of surface net charge. According to the above test, we used the (1×1) supercell with 17-layer symmetric slab geometry separated by 20 Å of vacuum space. The slabs are successively polarized with charges of $+0.222e$, $+0.444e$, $+0.667e$, $+0.889e$, $+1.111e$, $+1.333e$, $+1.556e$, $+1.778e$, and $+2.000e$. An $11 \times 11 \times 1$ k-point mesh is used, and CO is placed on both sides of these charged slabs to eliminate the dipole moment effects. The position of the central nine layers is fixed. The results are plotted in Fig. 8(b). It is clear that CO adsorption is nearly linearly dependent on the surface net charge, in good agreement with those shown in Fig. 3. This implicates that the more positive the Au atom is, the higher its d band is relative to the Fermi level, and the stronger CO adsorption will be.

- ¹B. Hammer and J. K. Nørskov, *Adv. Catal.* **45**, 71 (2000).
- ²J. J. Mortensen, B. Hammer, and J. K. Nørskov, *Phys. Rev. Lett.* **80**, 4333 (1998).
- ³Z. P. Liu and P. Hu, *J. Am. Chem. Soc.* **123**, 12596 (2001).
- ⁴T. S. Kim, J. Gong, R. A. Ojifinni, J. M. White, and C. B. Mullins, *J. Am. Chem. Soc.* **128**, 6282 (2006).
- ⁵R. A. Ojifinni, N. S. Froemming, J. Gong, M. Pan, T. S. Kim, J. M. White, G. Henkelman, and C. B. Mullins, *J. Am. Chem. Soc.* **130**, 6801 (2008).
- ⁶A. Bongiorno and U. Landman, *Phys. Rev. Lett.* **95**, 106102 (2005).
- ⁷P. J. Feibelman and D. R. Hamann, *Phys. Rev. Lett.* **52**, 61 (1984).
- ⁸C. H. Bartholomew, *Appl. Catal., A* **212**, 17 (2001).
- ⁹M. Rutkowski, D. Wetzig, and H. Zacharias, *Phys. Rev. Lett.* **87**, 246101 (2001).
- ¹⁰J. J. Mortensen, B. Hammer, and J. K. Nørskov, *Surf. Sci.* **414**, 315 (1998).
- ¹¹B. Hammer and J. K. Nørskov, *Nature (London)* **376**, 238 (1995).
- ¹²M. Haruta, T. Kobayashi, H. Sano, and N. Yamada, *Chem. Lett.* **16**, 405 (1987).
- ¹³A. K. Sinha, S. Seelan, S. Tsubota, and M. Haruta, *Top. Catal.* **29**, 95 (2004).
- ¹⁴M. D. Hughes, Y.-J. Xu, P. Jenkins, P. McMorn, P. Landon, D. I. Enache, A. F. Carley, G. A. Attard, G. J. Hutchings, F. King, E. H. Stitt, P. Johnston, K. Griffin, and C. J. Kiely, *Nature (London)* **437**, 1132 (2005).
- ¹⁵T. Ishida and M. Haruta, *Angew. Chem., Int. Ed.* **46**, 7154 (2007).
- ¹⁶B. Jorgensen, S. E. Christiansen, M. L. D. Thomsen, and C. H. Christensen, *J. Catal.* **251**, 332 (2007).
- ¹⁷N. Lopez and J. K. Nørskov, *J. Am. Chem. Soc.* **124**, 11262 (2002).
- ¹⁸N. Lopez, T. V. W. Janssens, B. S. Clausen, Y. Xu, M. Mavrikakis, T. Bligaard, and J. K. Nørskov, *J. Catal.* **223**, 232 (2004).
- ¹⁹Z. P. Liu, P. Hu, and A. Alavi, *J. Am. Chem. Soc.* **124**, 14770 (2002).
- ²⁰S. K. Shaikhutdinov, R. Meyer, M. Naschitzki, M. Baumer, and H. J. Freund, *Catal. Lett.* **86**, 211 (2003).
- ²¹C. Lemire, R. Meyer, S. Shaikhutdinov, and H. J. Freund, *Angew. Chem., Int. Ed.* **43**, 118 (2004).
- ²²B. K. Min, X. Deng, D. Pinnaduwage, R. Schalek, and C. M. Friend, *Phys. Rev. B* **72**, 121410(R) (2005).
- ²³G. C. Bond and D. T. Thompson, *Gold Bull.* **33**, 41 (2000).
- ²⁴B. Yoon, H. Hakkinen, U. Landman, A. S. Worz, J. M. Antonietti, S. Abbet, K. Judai, and U. Heiz, *Science* **307**, 403 (2005).
- ²⁵Z.-P. Liu, S. J. Jenkins, and D. A. King, *Phys. Rev. Lett.* **94**, 196102 (2005).
- ²⁶C. H. Christensen and J. K. Nørskov, *Science* **327**, 278 (2010).
- ²⁷A. Wittstock, V. Zielasek, J. Biener, C. M. Friend, and M. Baumer, *Science* **327**, 319 (2010).
- ²⁸J. A. Rodriguez, T. Jirsak, and S. Chaturvedi, *J. Chem. Phys.* **110**, 3138 (1999).
- ²⁹J. A. Rodriguez and J. Hrbek, *Acc. Chem. Res.* **32**, 719 (1999).
- ³⁰J. A. Rodriguez, J. Hrbek, M. Kuhn, T. Jirsak, S. Chaturvedi, and A. Maiti, *J. Chem. Phys.* **113**, 11284 (2000).
- ³¹Z. X. Yang, R. Q. Wu, and J. A. Rodriguez, *Phys. Rev. B* **65**, 155409 (2002).
- ³²J. A. Rodriguez, J. Dvorak, T. Jirsak, G. Liu, J. Hrbek, Y. Aray, and C. Gonzalez, *J. Am. Chem. Soc.* **125**, 276 (2003).
- ³³X. F. Hu and C. J. Hirschmugl, *Phys. Rev. B* **72**, 205439 (2005).
- ³⁴J. Oudar and H. Wise, *Deactivation and Poisoning of Catalysts* (Dekker, New York, 1991).
- ³⁵J. K. Lee and H. K. Rhee, *J. Catal.* **177**, 208 (1998).
- ³⁶W. Erley and H. Wagner, *J. Catal.* **53**, 287 (1978).
- ³⁷D. W. Goodman, IUCCP Conference, Texas A&M University, Texas, 1984, p. 230.
- ³⁸C. H. F. Peden and D. W. Goodman, in *Symposium on the Surface Science of Catalyst*, edited by M. L. Deviny and J. L. Gland (Philadelphia American Chemical Society, Washington, D.C., 1984), p. 185.
- ³⁹T. F. Zhang, Z. P. Liu, S. M. Driver, S. J. Pratt, S. J. Jenkins, and D. A. King, *Phys. Rev. Lett.* **95**, 266102 (2005).
- ⁴⁰L. Y. Gan, Y. X. Zhang, and Y. J. Zhao, *J. Phys. Chem. C* **114**, 996 (2010).
- ⁴¹L. Q. Xue, X. Y. Pang, and G. C. Wang, *J. Phys. Chem. C* **111**, 2223 (2007).
- ⁴²P. Mohapatra, J. Moma, K. M. Parida, W. A. Jordaan, and M. S. Scurrill, *Chem. Commun. (Cambridge)* **2007**, 1044.
- ⁴³K. Kershen, H. Celio, I. Lee, and J. M. White, *Langmuir* **17**, 323 (2001).
- ⁴⁴R. W. Gurney, *Phys. Rev.* **47**, 479 (1935).
- ⁴⁵S. J. Jenkins and D. A. King, *Chem. Phys. Lett.* **309**, 434 (1999).
- ⁴⁶G. Kresse and J. Hafner, *Phys. Rev. B* **47**, 558 (1993).
- ⁴⁷G. Kresse and J. Hafner, *Phys. Rev. B* **48**, 13115 (1993).
- ⁴⁸G. Kresse and J. Furthmuller, *Comput. Mater. Sci.* **6**, 15 (1996).
- ⁴⁹G. Kresse and J. Furthmuller, *Phys. Rev. B* **54**, 11169 (1996).
- ⁵⁰P. E. Blöchl, *Phys. Rev. B* **50**, 17953 (1994).
- ⁵¹G. Kresse and D. Joubert, *Phys. Rev. B* **59**, 1758 (1999).
- ⁵²J. P. Perdew and W. Yue, *Phys. Rev. B* **33**, 8800 (1986).
- ⁵³J. P. Perdew, J. A. Chevary, S. H. Vosko, K. A. Jackson, M. R. Pederson, D. J. Singh, and C. Fiolhais, *Phys. Rev. B* **46**, 6671 (1992).
- ⁵⁴C. Kittel, *Introduction to Solid State Physics* (Wiley, NY, 1986).
- ⁵⁵N. Al-Sarraf, J. T. Stuckless, and D. A. King, *Nature (London)* **360**, 243 (1992).
- ⁵⁶E. Wimmer, C. L. Fu, and A. J. Freeman, *Phys. Rev. Lett.* **55**, 2618 (1985).
- ⁵⁷P. He and K. Jacobi, *J. Chem. Phys.* **106**, 3417 (1997).
- ⁵⁸S. J. Jenkins and D. A. King, *J. Am. Chem. Soc.* **122**, 10610 (2000).
- ⁵⁹S. J. Pratt and D. A. King, *Surf. Sci.* **540**, 185 (2003).
- ⁶⁰R. Bader, *Atoms in Molecules: A Quantum Theory* (Oxford University Press, New York, 1990).
- ⁶¹B. Hammer and J. K. Nørskov, *Surf. Sci.* **343**, 211 (1995).
- ⁶²G. Mills, M. S. Gordon, and H. Metiu, *J. Chem. Phys.* **118**, 4198 (2003).
- ⁶³A. Politano, V. Formoso, and G. Chiarello, *Appl. Surf. Sci.* **254**, 6854 (2008).
- ⁶⁴A. Politano, R. G. Agostino, V. Formoso, and G. Chiarello, *ChemPhysChem* **9**, 1189 (2008).
- ⁶⁵S. Stolbov and T. S. Rahman, *Phys. Rev. Lett.* **96**, 186801 (2006).
- ⁶⁶L. Chen, B. Chen, C. Zhou, J. Wu, R. C. Forrey, and H. Cheng, *J. Phys. Chem. C* **112**, 13937 (2008).

Erratum: “Charge effect in S enhanced CO adsorption: A theoretical study of CO on Au, Ag, Cu, and Pd (111) surfaces coadsorbed with S, O, Cl, and Na” [J. Chem. Phys. 133, 094703 (2010)]

Li-Yong Gan and Yu-Jun Zhao^{a)}

Department of Physics and School of Material Science and Engineering, South China University of Technology, Guangzhou 510640, People's Republic of China

(Received 14 January 2011; accepted 18 January 2011; published online 9 February 2011)

[doi:10.1063/1.3553260]

In the original version of the article,¹ some figure legends are missing in Figs. 4(a)–4(c), and therefore, Fig. 4 should be updated to the revised version as follows:

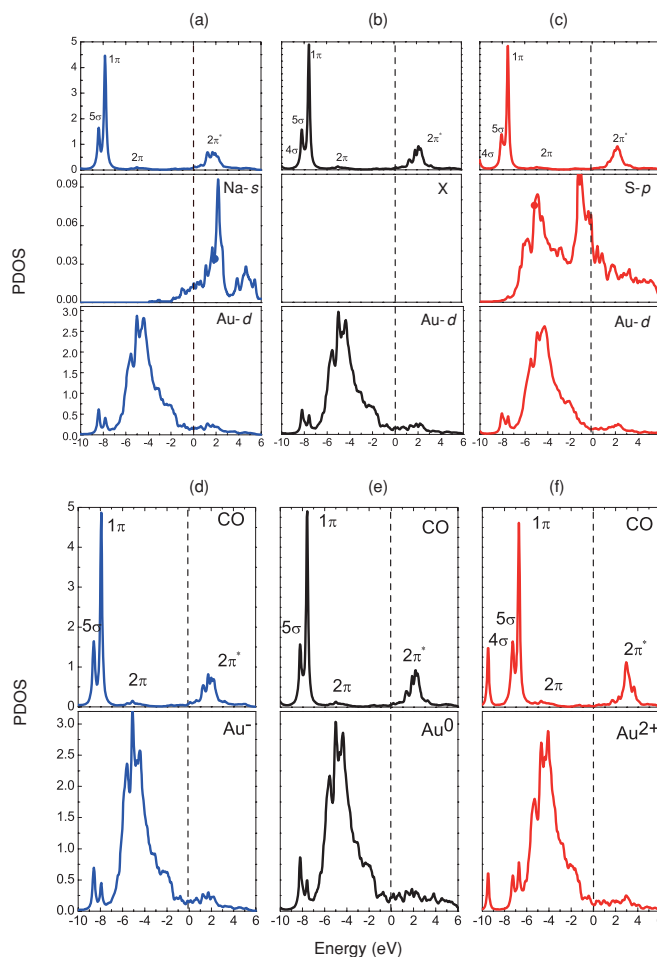


FIG. 4.

¹L.-Y. Gan and Y.-J. Zhao, *J. Chem. Phys.* **133**, 094703 (2010).

^{a)} Author to whom correspondence should be addressed. Electronic mail: zhaoyj@scut.edu.cn. Tel: +86-20-87110426. Fax: +86-20-87112837.